

# Climate Change in Eastern Victoria

Stage 1 Report:

The effect of climate change on coastal  
wind and weather patterns



*A Project Undertaken for the Gippsland Coastal Board*

*by*

*K.L. McInnes, D. J. Abbs, & J. A. Bathols*

*CSIRO Marine and Atmospheric Research*

*June 2005*

K.L. McInnes, D. J. Abbs, & J. A. Bathols

**CSIRO Marine and Atmospheric Research**

**Consultancy report for the Gippsland Coastal Board**

© CSIRO 2005

### ***Important Disclaimer***

---

*This report relates to climate change scenarios based on computer modelling. Models involve simplifications of the real physical processes that are not fully understood. Accordingly, no responsibility will be accepted by CSIRO for the accuracy of projections in this report or actions on reliance of this report.*

---

*Address for correspondence*

*Kathleen McInnes*

*CSIRO Marine and Atmospheric Research  
PMB No 1, Aspendale, Victoria, 3195  
Telephone (03) 9239 4660  
Fax (03) 9239 4444  
E-mail Kathleen.McInnes@csiro.au*

CSIRO Marine and Atmospheric Research (<http://www.cmar.csiro.au>) provides scientific advice and solutions on issues involving the atmospheric environment, the climate system, coastal management, sustainable marine resources and industry. Our work is directed toward meeting the needs of government, industry and the community.

*For more information about climate change, see  
<http://www.dar.csiro.au/information/climatechange.html>*

## Table of Contents

Executive Summary .....	5
1 Introduction.....	7
2 Overview of Project Methodology.....	7
3 Wind Projections .....	8
3.1 Model Selection .....	8
3.2 Global Patterns of Change.....	9
3.3 Projected Changes in Wind Speed.....	10
4 Extreme Weather Events .....	15
4.1 Data Sets and Event Selection .....	16
4.2 Extreme Wind Synoptic Weather Types .....	17
4.3 Extreme Sea Level Synoptic Weather Patterns .....	19
4.4 The Impact of Climate Change .....	21
5 Summary .....	22
Acknowledgments .....	23
References	24
Appendix 1 – Synoptic Typing.....	25



## Executive Summary

This report presents the results of the first stage of a study in which storm surge return periods are evaluated along the eastern Victorian coast under late twentieth century climate conditions and climate conditions that may be realised during the course of the 21<sup>st</sup> century. Storm surges along the eastern Victorian coastline are caused by severe winds and, to a lesser degree, the associated falling atmospheric pressure that accompanies them. This report presents an assessment of climate model simulations in terms of changes to wind conditions and the synoptic weather events that are conducive to storm surge formation. This will provide the basis for generating atmospheric data with which to force a storm surge model in stage 2 of the study.

### Mean Wind Projections

Based on thirteen climate model simulations, future changes in mean 10 m winds were found to contain large uncertainty. There was strong seasonality in the changes with a tendency towards increases over southeastern Victoria, Bass Strait and the southern Tasman Sea in winter and spring, weak increases in summer and decreases in autumn. The ranges of change as a percentage relative to the average 1961 to 1990 conditions are summarised as follows:

Season	<i>Melbourne to Wilson's Prom</i>		<i>Wilson's Prom to NSW border</i>	
	2030 %	2070 %	2030 %	2070 %
Summer	-1 - +5	-4 - +16	-1 - +3	-4 - +8
Autumn	-4 - +1	-12 - +4	-4 - +1	-12 - +4
Winter	-4 - +5	-12 - +16	-1 - +5	-4 - +16
Spring	-3 - +4	-8 - +12	-3 - +4	-8 - +12

### Extreme Wind Projections

Future changes in the 95<sup>th</sup> percentile 10 m winds are more uncertain than those in mean 10m winds. The ranges of change are summarised below. In some cases, where ranges varied within a region, the more conservative (larger) range has been given.

Season	<i>Melbourne to Wilson's Prom</i>		<i>Wilson's Prom to NSW border</i>	
	2030 %	2070 %	2030 %	2070 %
Summer	-5 - +5	-16 - +16	-5 - +5	-16 - +16
Autumn	-10 - +5	-32 - +10	-10 - +5	-32 - +10
Winter	-3 - +8	-8 - +24	-6 - +10	-16 - +32
Spring	-5 - +5	-16 - +16	-5 - +5	-16 - +16

### Extreme Weather Events

A synoptic typing procedure has been used to identify the weather systems responsible for severe winds and elevated sea level conditions along the eastern Victorian coast. An analysis of the strongest 1% of winds in Bass Strait and the southern Tasman Sea for the 1961 to 2000 period yielded six synoptic weather patterns that were named prefrontal, frontal, post-frontal, Tasman low, cut-off low and continental low. The dominant wind directions through eastern Bass Strait that are associated with the prefrontal pattern are northwesterly, shifting to westerly or southwesterly for frontal and post-frontal events. Tasman lows are associated with southerly to southeasterly winds while cut-off lows result in southeasterly to easterly winds. Continental lows are generally associated with easterlies. The three stages of frontal events were the most frequently occurring patterns,

accounting for 69% of severe wind days. Tasman lows accounted for 23% of severe wind days, cut-off lows accounted for 6% and continental lows accounted for 2%.

Tide gauge data with the tidal component removed yields residuals that provide information about the influence of weather on sea levels. Tide gauge residual data at Stony Point near Western Port Bay and at Lakes Entrance were used to identify dates on which storm surges occurred, the synoptic patterns of which were correlated against the six severe wind standard types. A daily maximum sea level residual value of 0.4 m or greater was used as a threshold for storm surge identification. The procedure identified that about 96% of elevated storm surge events at Stony Point were due to the passage of cold fronts while only 1% was due to Tasman lows. Elevated sea levels at Lakes Entrance were caused by fronts in about 71% of occasions, Tasman lows in about 23% of cases and cut-off lows in about 3% of cases.

Future changes in the frequencies of synoptic weather patterns were examined using two high resolution (approximately 60 km) regional climate model simulations performed using the CSIRO Cubic Conformal (CC) model, one embedded within the CSIRO Mark 2 global climate model and one embedded in the CSIRO Mark 3 global climate model. Of the two models, the CC-Mk2 model more closely reproduced the proportion of weather patterns associated with severe winds over eastern Victoria and Bass Strait found in the observations, whereas the CC-Mk3 model produced a higher number of frontal events, fewer Tasman Lows and a greater percentage of patterns that could not be classified according to the six standard types. The number of frontal days contributing to the most severe 1% of wind days increases in the CC-Mk2 from 72% during a 1961 to 1990 reference period to 77% in 2030 and 79% by 2070. Cut-off lows, on the other hand, declined from 6% to 4% in 2030 and to 3% by 2070. Tasman lows also decline slightly from 17% to 16% by 2070. In the CC-Mk3 model, frontal conditions are found to decrease slightly from 86% over the reference period to 83% in 2030 and 82% in 2070 while cut-off lows show a small increase in frequency.

The analysis of the nature of the synoptic events responsible for storm surges along the eastern Victorian coast and the projections of future changes in their relative frequencies and associated wind speeds will form the basis for the generation of atmospheric data with which to force a storm surge model in stage 2 of the study.

## 1 Introduction

This report has been prepared in response to a request from the Gippsland Coastal Board for specific information on the impact of climate change in relation to regional sea level rise and anticipated changes to weather patterns (e.g. frequency and intensity of storms) along the eastern Victorian coast and the subsequent impacts of these upon the frequency of storm surges. The results of this study provide a basis for assessing the impact of sea level change on the geomorphology and physical assets along the Gippsland Coast.

A two-stage research program has been designed and this report details the results of stage 1 in which a general assessment is undertaken into possible changes in the wind and weather patterns that drive coastal processes such as waves and storm surges. Stage 2 will comprise a comprehensive evaluation of changes in storm surge return periods. The information provided in the two stages will provide information for subsequent impacts assessment.

The goal of this project is to provide spatial maps of storm surge return periods under present and future climate conditions for the eastern Victorian coast from about Inverloch to the NSW border. The methodology involves the use of a hydrodynamic model to simulate elevated sea levels along the coast and these simulations are analysed to produce sea level recurrence intervals. The upper boundary of the domain of the hydrodynamic model is the sea surface, for which atmospheric data must be provided. The results of the first stage of the project provide the basis for the provision of this data.

For present climate conditions, the properties of the synoptic weather conditions that cause increases in coastal sea levels are investigated. The need to include the effects of climate change requires additional analysis of climate models to evaluate not only how wind speed may change in the future, but how the frequencies and intensities of the different synoptic weather events associated with extreme sea levels may be affected.

## 2 Overview of Project Methodology

The assessment of future weather patterns proposed comprises three parts:

*(i) Scenarios of mean near-surface winds*

These are based on projected wind speed changes from a range of climate models both from CSIRO and other international research organisations. They are provided as ranges of possible change that span the uncertainty associated with the projections over the given geographical domain based on the methodology for outlined in Whetton et al (in preparation), recent examples of which can be found in Hennessy et al (2004a, b).

*(ii) Development of scenarios of extreme near-surface winds*

The method used for the mean near surface wind is further developed to provide projections for the top 5% of wind speeds.

*(iii) Analysis of the classes of extreme weather events*

Extreme sea level events along the eastern Victorian coastline are driven primarily by two classes of synoptic weather system, those originating from the west in the form of cold fronts and those originating from the east such as east coast lows. Further

analysis of model output determines how the model represents each of these contributors to extreme sea levels under present climate conditions and how these change in the future in terms of their frequency and severity.

The results of the above analyses are to form the basis of atmospheric data sets representing severe near-surface weather conditions responsible for storm surges along Victoria's eastern coastline under current and future climate conditions. In stage 2 of the project, these data sets will be used as the forcing for a coastal ocean model capable of simulating coastal currents and sea level variations due to tides and storm surge. Spatially varying storm tide return periods will be calculated from the output of this coastal model.

### 3 Wind Projections

Projected changes in wind patterns across eastern Victoria were analysed in a range of climate model simulations following the methodology described in Whetton et al (in preparation). Scenarios of average and extreme wind conditions are presented and discussed.

#### 3.1 Model Selection

A wide range of climate simulations from international modelling groups are available to CSIRO for developing regional climate projections. A summary of the 20 available sets of simulations is given in Table 2. Note that for some models there exists an older simulation conducted using an emissions scenario based on IS92a or a 1% per annum compounding increase in CO<sub>2</sub> as well as the more recent simulations carried out using various different SRES scenarios (see IPCC, 2000). These simulations were subjected to quality control procedures leading to the exclusion of several poorer performing models from the scenarios. The excluded models were CCSRNIES, ECHAM3, GFDL.1 and NCARCSM. Simulations from ten global models and three regional models were retained.

**Table 2:** Climate model simulations analysed in this report. Note that D125 and CC are Regional Climate Models. Further information about the non-CSIRO simulations may be found at the IPCC Data Distribution Centre (<http://ipcc-ddc.cru.uea.ac.uk>).

Centre	Model	Emissions Scenarios post-1990 (historical forcing prior to 1990)	Years	Horizontal resolution (km)
Canadian CC	CCCM1	1% increase in CO <sub>2</sub> p.a.	1900–2100	~400
Canadian CC	CCCM2	IS92a	1961-2100	~400
Canadian CC	CCCM2	CO <sub>2</sub> + aerosol SRES, A2, B2	1900-2100	~400
CCSR, Japan	CCSRNIES	SRES, A1, A1F1,A1T,A2,B1,B2	1890-2100	~500
CSIRO, Aust	Mark2.1	IS92a	1881–2100	~400
CSIRO, Aust	Mark2.2	SRES A2 (four simulations), SRES B2	1881–2100	~400
CSIRO, Aust	DARLAM	IS92a	1961-2100	125
CSIRO, Aust	Mark3	SRES A2	1961-2100	~200
CSIRO, Aust	CCMk2	Mark 2 SRES A2	1961-2100	~60
CSIRO, Aust	CCMk3	Mark 3 SRES A2	1961-2100	~60
DKRZ, Germany	ECHAM3/LSG	IS92a	1880-2085	~600
DKRZ, Germany	ECHAM4/OPYC3.1	IS92a	1860–2099	~300
DKRZ Germany	ECHAM4/OPYC3.2	CO <sub>2</sub> +O <sub>3</sub> + aerosol, SRES A2, B2	1990-2100	~300
GFDL	GFDL.1	1% increase in CO <sub>2</sub> p.a.	1958–2057	~500
GFDL	GFDL.2	Varying insolation + aerosol, SRES A2, B2	1961-2100	~500
Hadley Centre, UK	HadCM2	1% increase in CO <sub>2</sub> p.a. (four simulations)	1861–2100	~400
Hadley Centre, UK	HadCM3.1	IS92a	1861-2099	~400
Hadley Centre, UK	HadCM3.2	CO <sub>2</sub> +O <sub>3</sub> + aerosol, SRES, A2, B2	1950-2099	~400
NCAR –CSM	NCARCSM	SRES A2	2000-2099	~300
NCAR-PCM	NCARPCM	CO <sub>2</sub> + aerosol SRES, A1B, A2, B2	1980-2099	~300

### 3.2 Global Patterns of Change

It is instructive to examine the broad patterns of change simulated by the models in variables such as winds and pressure to provide a context for understanding the changes on the local scale. Figure 1 represents the agreement between models on changes in near-surface wind speed across the globe using the ten selected global climate models (note that the three regional models are omitted from this analysis). While the magnitude of the change is generally small (less than 3% per degree of global warming), there is agreement between models on changes across a large part of the globe. Increases in wind speed occur over the Southern Ocean south of about 50°S. Increases in wind speed are also indicated over the southern Tasman Sea and across the Australian mainland. Changes are less certain immediately to the southwest of Tasmania while decreases are indicated over the Bight and extend into the Indian Ocean.

The change in wind pattern in the southern hemisphere is strongly related to the pattern of pressure change (Figure 2) with the band of increasing winds in the Southern Ocean overlapping and extending slightly to the north of a band of decreasing pressure. Decreasing pressure is also indicated across inland Australia while increasing pressure occurs to the south and west of Australia and across the southern Pacific Ocean.

The pattern of pressure change in the southern hemisphere is one of increasing pressure in the vicinity of the sub-tropical ridge and decreasing pressure in the sub-polar trough which leads to stronger winds in the regions between. The reason for this pattern of change is not well understood, but there is evidence that the tendency toward increased pressure in the 40-60°S latitude band is related to a delayed warming in southern high latitudes due to the downward transport of heat by the ocean (see Whetton et al, 1996). There is also some agreement amongst models on decreased pressure over Australia. Both these features are also present in seasonal analyses (not shown), with the increased pressure band extending slightly further north in winter and the pressure decreases over the Australian continent being greater in summer.

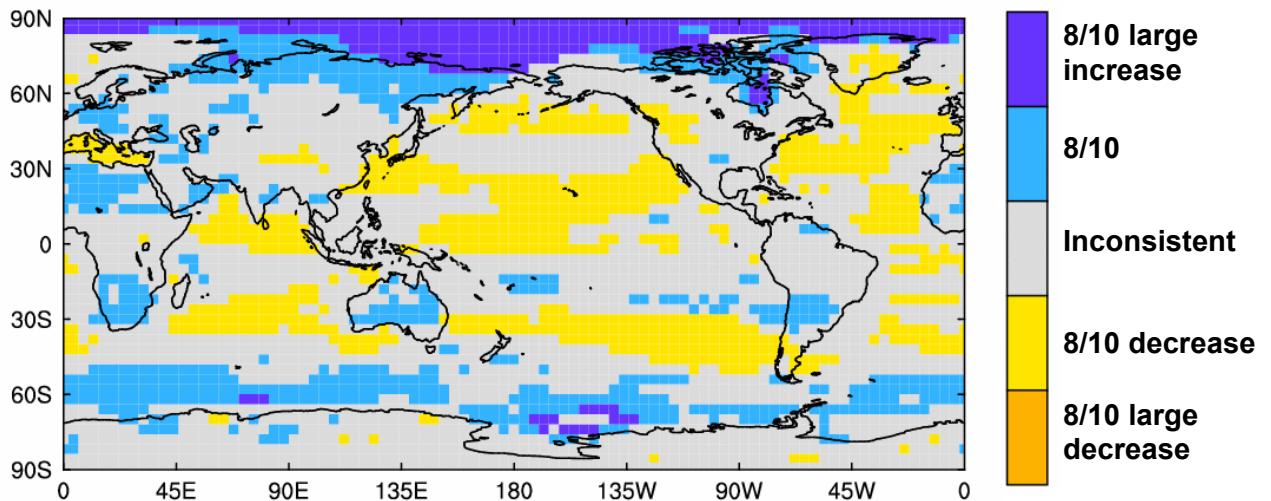


**Figure 1:** Agreement between ten models regarding changes in annual near-surface wind speed. Large changes are defined as being those greater than 3% per °C of global warming.

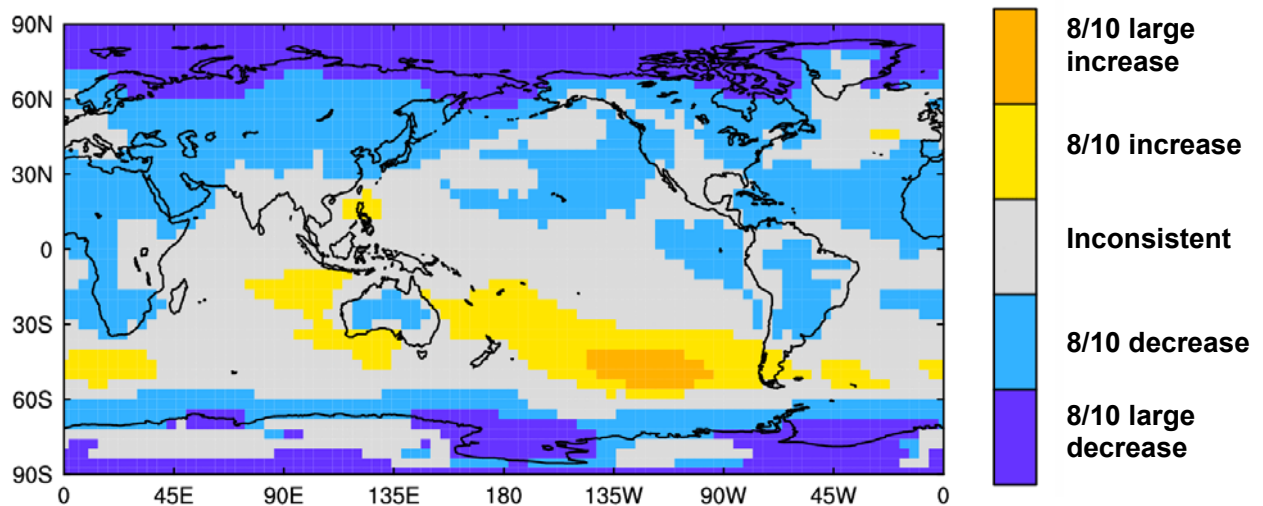


**Figure 2:** Agreement between ten models regarding changes in annual pressure change. Large changes are defined as being those greater than 50 Pa per °C of global warming.

### 3.3 Projected Changes in Wind Speed

Scenarios of wind speed changes were developed for two future years from the thirteen patterns of change per degree of global warming by multiplying the patterns by the range of global warming projected at the particular future year. Three different emissions scenarios were included in the projections:

- the IPCC SRES scenarios without policies to reduce greenhouse gas emissions;
- the IPCC scenario for stabilising atmospheric CO<sub>2</sub> concentrations at 550 ppm by the year 2150;
- the IPCC scenario for stabilising atmospheric CO<sub>2</sub> concentrations at 450 ppm by the year 2090.

Scenarios of changes in wind speed over eastern Victoria are presented in Figures 3 and 5 as colour-coded maps representing the range of possible change. The colour coding indicates the quantifiable uncertainties associated with:

- scenarios of future emissions in greenhouse gases and aerosols;
- the climate sensitivity, i.e. the amount of global warming that will occur for given atmospheric concentrations of greenhouse gases;
- differences between the climate model simulations in terms of regional climate change.

The ranges of change for the two IPCC stabilisation scenarios are narrower than those for the SRES scenarios. The discussion of results in this section is limited to the ranges of future change under the SRES scenarios and to the coastal region between Melbourne and the New South Wales border.

#### 3.3.1 Changes in mean wind speed

Mean wind speed changes across eastern Victoria, shown in Figure 3, contain large uncertainty in all seasons in that all seven of the possible ranges of change are ranges that span zero change. However, some ranges tend more towards increases than decreases as is the case for coastal Victoria and Bass Strait in summer, winter and spring.

In summer, the mean wind speed change between Melbourne and Wilson's Promontory is in the range of -1 to +5% in 2030 and -4 and +16% in 2070 while between Wilson's Prom and the border, it lies in a narrower range, between -1 and +3% in 2030 and -4 and +8% by 2070. During autumn, there is a tendency toward decreases in mean wind speed in the range of -4 to +1% in 2030 and -12 to +4% in 2070 over eastern Victoria, Bass Strait and the southern Tasman Sea. In winter, changes between Melbourne and Wilson's Prom are in the range of -4 to +5% in 2030 and -12 to +16% in 2070. These transition to changes in the range of -1 to +5% in 2030 and -4 to +16% in 2070 east of Wilson's Prom. A region in western Bass Strait exists where the lower limit decreases to -4% in 2030 and -12% in 2070. In spring, changes in mean wind speed to the west of Wilson's Prom are in the range -4 to +5% in 2030 and -12 to +16% in 2070. To the east of this, changes are mainly in the range -3 to +4% in 2030 and -8 to +12% in 2070.

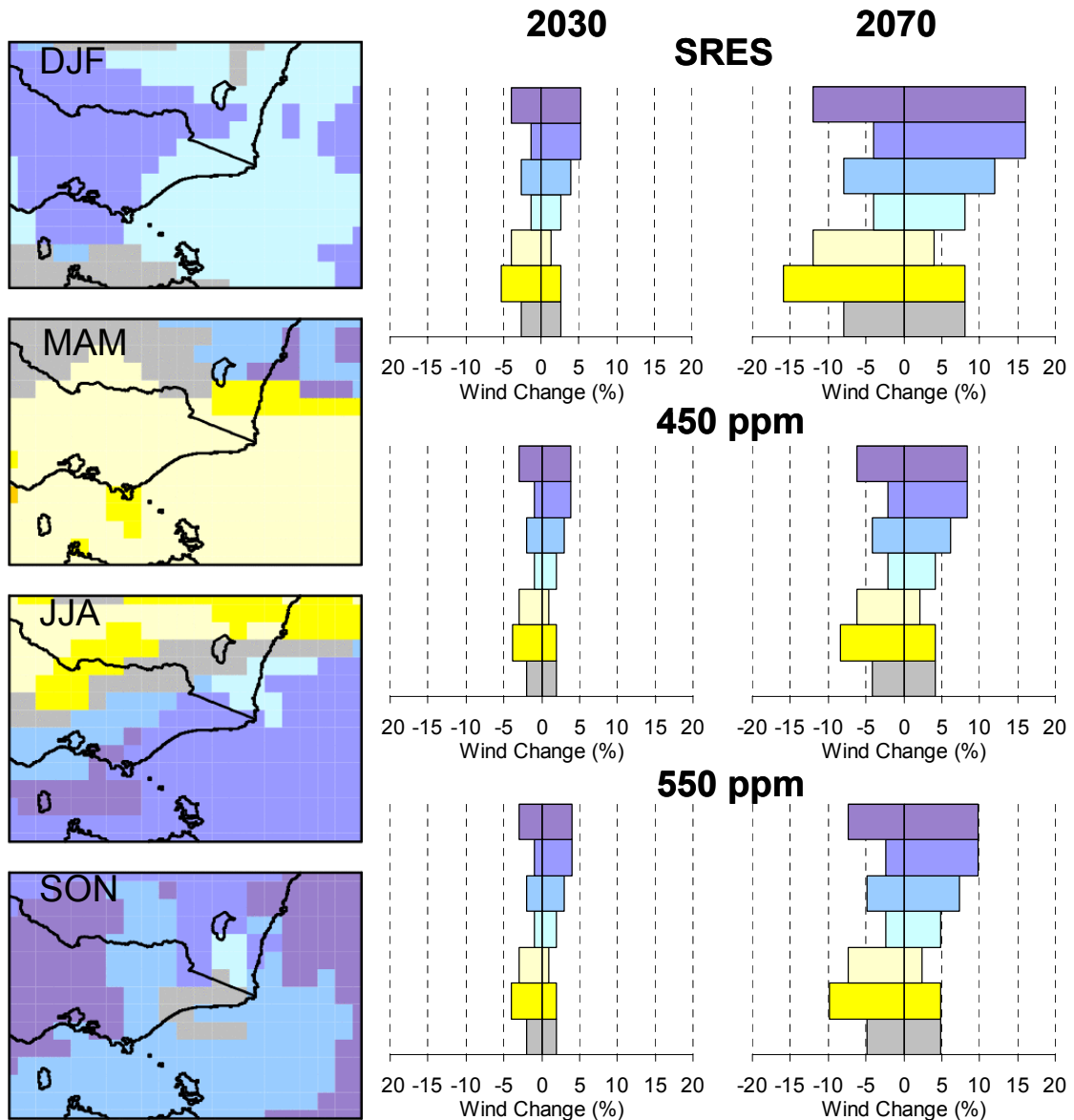


**Figure 3:** Ranges of change in mean near-surface (10 metres above ground) wind speed for the years 2030 and 2070 relative to the 1961 to 1990 average. The coloured bars show ranges of change for areas with corresponding colours in the maps. The IPCC SRES scenarios do not include explicit actions to reduce greenhouse gas emissions. Ranges are also shown for the IPCC's 550 ppm and 450 ppm CO<sub>2</sub> stabilisation scenarios. DJF = summer, MAM = autumn, JJA = winter, SON = spring.

The projections in Figure 3 convey information about the range of change but no information on the likelihood of any particular change taking place. In the absence of probabilistic projections, and in view of the fact that for wind speed both increases and decreases are possible, it is informative to also present the wind speed change averaged over the thirteen model simulations noting that there is large uncertainty in doing this. The average wind speed change (Figure 4a) shows strong qualitative similarity to the projections in Figure 3 in that areas that had a range of change that was biased towards a particular sign shows an average change in the same direction. Note that the averages in Figure 4 have not been scaled to represent a particular future date under a warming scenario and so the units are percentage change per degree of global warming. To eliminate the dependency on global warming, these values need to be multiplied by a global warming value. For example, the global warming range due to emissions uncertainty and climate sensitivity is, for the SRES scenarios, 0.4 to 1.0°C in 2030 and 1.1 to 4.0°C in 2070.

Figure 4b presents the number of model simulations, out of the thirteen considered, that agree on an increase in wind. This provides information on whether the ranges of change are influenced by a majority of the models or are dominated by outlier results from a minority of models. It can be seen that there is broad consistency between the sign of the average changes and the number of models simulating the particular direction of the changes. Exceptions occur to the south of the mainland in summer and over Bass Strait and southeastern Victoria in spring where, although the average of the thirteen models indicate increasing winds, this is due to a relatively large increase in winds simulated by a minority of the models.

### *3.3.2 Changes in extreme wind speeds*

The results described in this section are based on data from the same thirteen climate model simulations used for the analysis of mean wind speeds. Monthly averaged values of wind speeds have been considered since daily wind speeds were only available from the CSIRO models.

In the analysis, an extreme wind speed is defined as a speed above the 95<sup>th</sup> percentile for the sample of speeds in question. The 95<sup>th</sup> percentile for monthly wind speeds for a given month in a given year was determined by considering monthly speeds for all of the months in the appropriate seasons within a seven year window centred on the year of interest. This yielded 21 monthly wind speeds that could be ranked, with the highest ranking wind speed equating to the 95<sup>th</sup> percentile.

Projections for the extreme wind speeds are shown in Figure 5. As with the mean wind speed projections, the discussion of the extreme wind speeds will focus on the SRES scenarios for 2030 and 2070, acknowledging that changes in wind speed under the CO<sub>2</sub> stabilisation scenarios have smaller ranges of uncertainty. Only three ranges tended towards increases in wind speed, two towards decreases and two were centred on zero with different ranges of uncertainty. The maximum range of change for the extreme wind speeds was from -10 to +10% for 2030 and -31 to +31% for 2070 under the SRES scenarios. This is approximately double the range of change for mean wind speeds, which suggests that wind speeds in the region of interest will become more variable under at least some of the SRES scenarios.

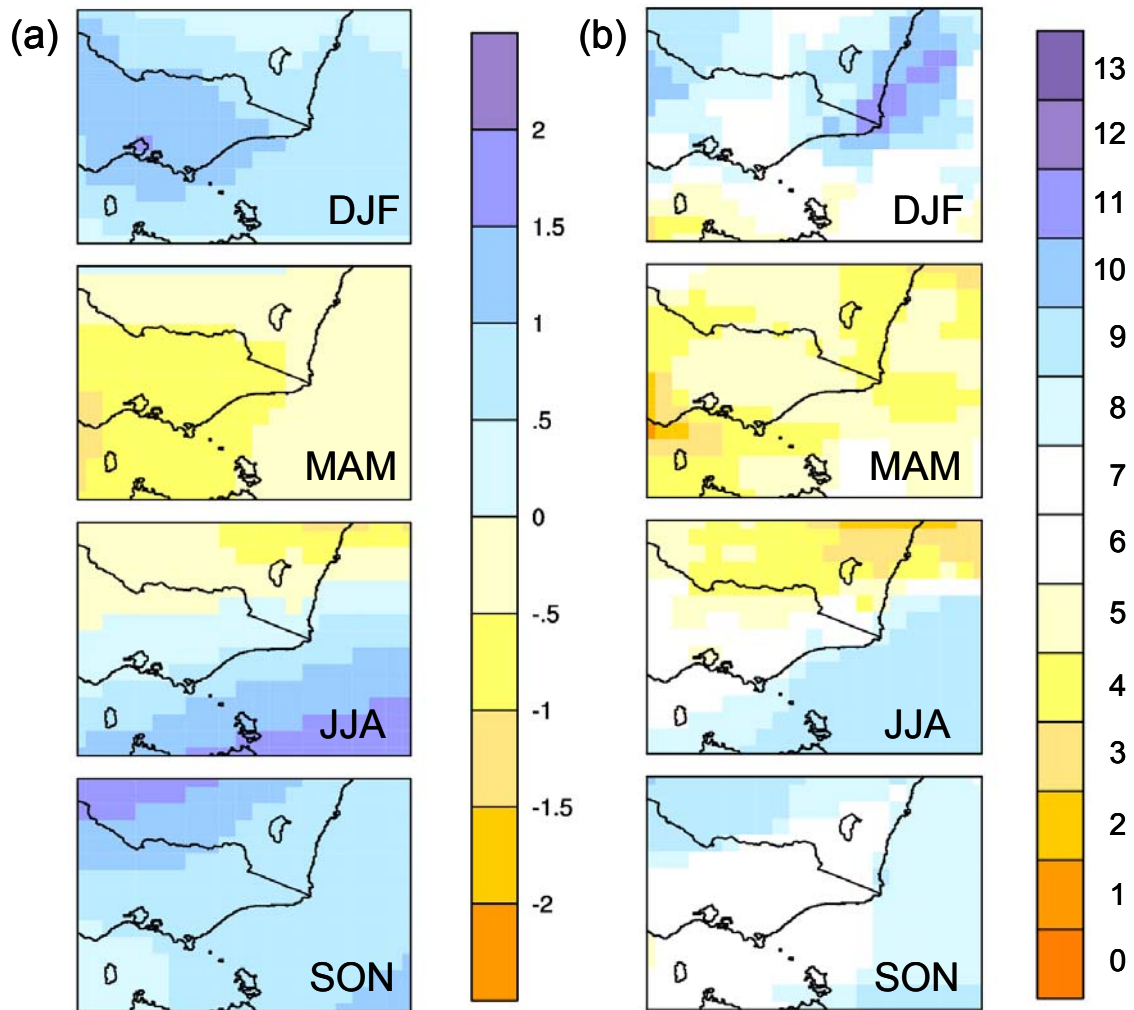


**Figure 4:** (a) The average change in mean wind speed derived by averaging the results from the thirteen model simulations. (% change per °C of global warming). (b) The number of models agreeing on an increase in wind speed. The scale can be reversed to indicate the number of models agreeing on a decrease in wind speed.

During summer and spring, changes in extreme wind speeds are in the range of -5 to +5% in 2030 and -16 to +16% in 2070 over most of the coast from Melbourne to the NSW border although results in these seasons are very noisy with the upper limit of change increasing in places to +8% by 2030 and +24% by 2070. In autumn there is a marked tendency towards a decrease in wind speed in the range of -10 to +5% in 2030 and -32 to +16% in 2070. In winter there is a tendency towards increasing wind speed in the range of -3 to +8% in 2030 and -8 to +24% in 2070 from Melbourne to Sale and -3 to +10% in 2030 and -8 to +32% in 2070 to the east of Sale.

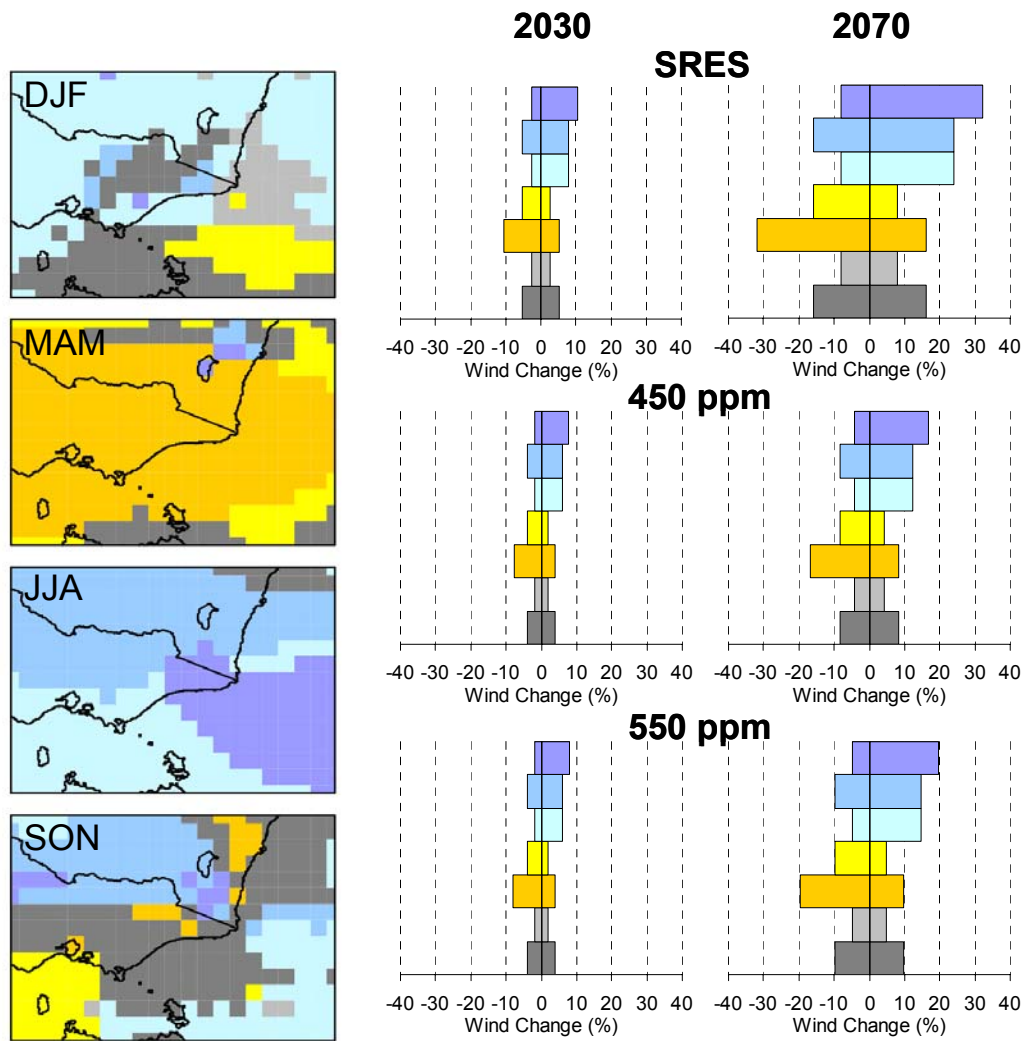


**Figure 5:** Ranges of change in extreme near-surface (10 metres above ground) wind speed for the years 2030 and 2070 relative to the 1961 to 1990 average. The coloured bars show ranges of change for areas with corresponding colours in the maps. The IPCC SRES scenarios do not include explicit actions to reduce greenhouse gas emissions. Ranges are also shown for the IPCC's 550 ppm and 450 ppm CO<sub>2</sub> stabilisation scenarios. DJF = summer, MAM = autumn, JJA = winter, SON = spring.

As with mean wind speeds, the extreme wind speeds are also presented averaged over the thirteen model simulations in Figure 6a. This reveals an average increase in wind speeds in summer and winter over eastern Victoria. In winter, there is a positive gradient in wind speed change between central Victoria, where changes do not exceed 0.5% per degree of global warming, to the southern Tasman Sea, where changes exceed 1.5% per degree. In autumn, average decreases in wind occur. In spring small average increases occur over the southern Tasman Sea with decreases over southern Victoria and Bass Strait. The largest offshore increases in average wind speeds to the southeast of the continent in summer and winter occur in the majority of models. Other increases in Victoria, Bass Strait and the Tasman Sea are generally due to relatively large increases occurring in a minority of models. In autumn and spring, as with summer and winter, the results are broadly similar to those obtained for mean wind speeds showing that in this region the behaviour of extreme wind speeds is similar to that of the mean wind speeds under enhanced greenhouse conditions.

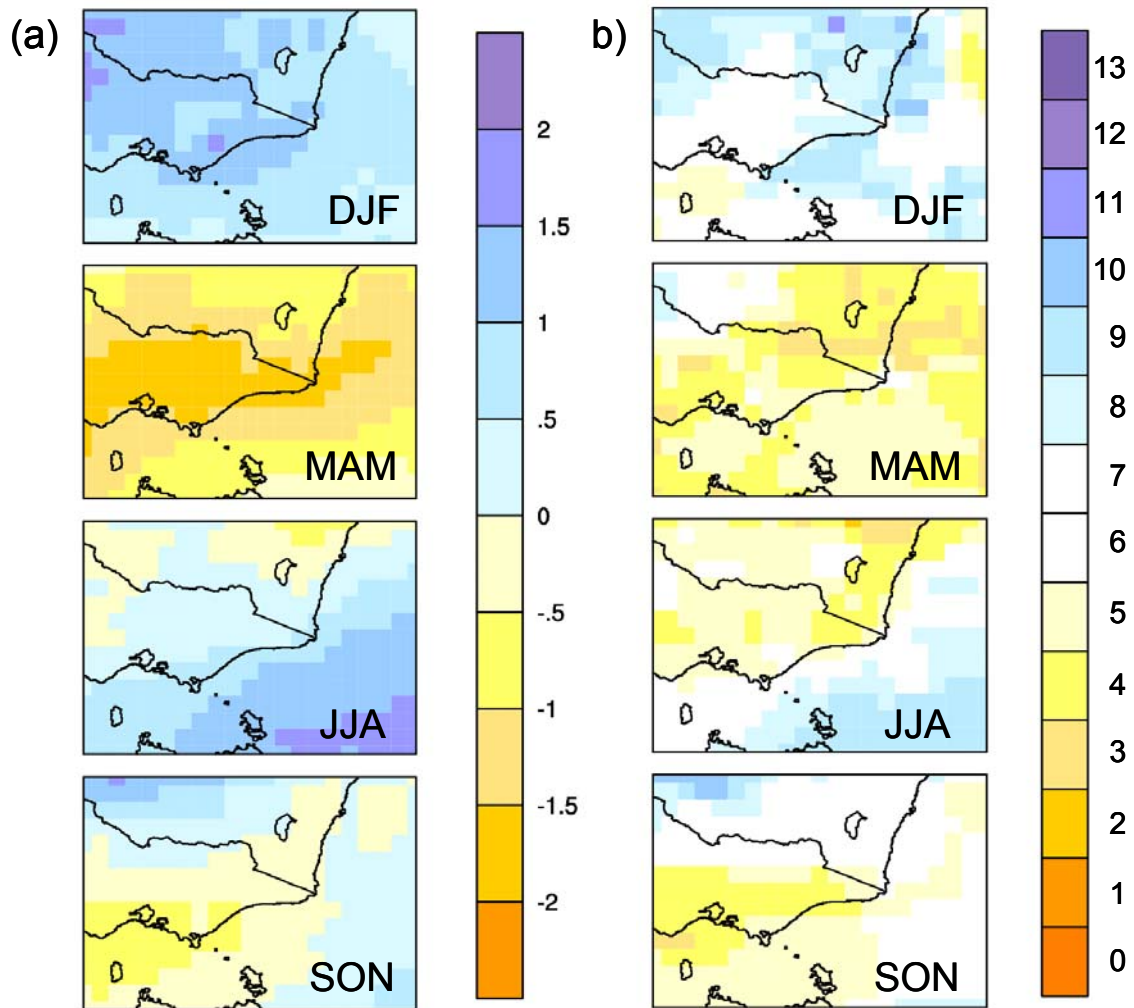


**Figure 6:** (a) The average change in extreme wind speed derived by averaging the results from thirteen simulations. (% change per °C of global warming). (b) The number of models agreeing on an increase in winds. The scale can be reversed to indicate the number of models agreeing on a decrease in winds.

#### 4 Extreme Weather Events

This chapter discusses the severe weather events responsible for elevated sea level events along the eastern Victorian coast and the impact of climate change on these events. A synoptic typing procedure that identifies similarities in daily analyses of sea level pressure is applied to reanalysis data and output from climate model simulations over the period covered by reanalysis data and selected future periods. Although the focus of the study is on weather events that produce elevated sea levels, such events are identified using a wind speed threshold since elevated sea level events are not simulated in climate models. Once the dominant synoptic weather patterns have been identified the relationships between these patterns and the occurrence of elevated sea levels at two tide gauges within the region of interest are then examined. This information will be used to formulate a relationship between sea level extremes, wind speed extremes and synoptic weather patterns which will be used to determine how climate change may affect

the synoptic events responsible for elevated sea levels along the eastern Victorian coast in stage 2 of the project.

#### **4.1 Data Sets and Event Selection**

The data set used for the analysis of extreme wind speeds is the National Centers for Environmental Prediction (NCEP) reanalysis data set. The NCEP reanalyses consist of the output of a global numerical weather prediction model into which all available global weather observations throughout the simulation period have been assimilated. The output of the model is dominated by the observations over the regions for which observations are available and provides a dynamically consistent representation of the atmosphere over data sparse parts of the globe. The 10 m wind speeds from this data set are available in a gridded format at a horizontal resolution of approximately  $1.9^{\circ} \times 1.9^{\circ}$  every six hours from 1958 to the present.

In the present study, the wind data are analysed on a once daily basis over the 40-year period from 1961 to 2000. The use of once daily wind data is to align the analysis of observed winds with those of the climate model in which winds are available only once per day of the simulation.

Mean sea level pressure (MSLP) reanalysis data have been used to characterise the synoptic scale weather systems that are conducive to extreme wind speeds in the study region. The MSLP data are available in a gridded format at a horizontal resolution of approximately  $2.5^{\circ} \times 2.5^{\circ}$  every six hours from 1958 to the present. In this study the MSLP data have been analysed once daily for the extreme wind speed events.

Fields of once daily 10 m wind speed and MSLP from CSIRO CC-Mk2 and CC-Mk3 climate model simulations were also analysed. These Cubic Conformal (CC) models represent the globe with a stretched grid in which the earth is mapped onto a cube. The mapping is such that higher resolution is focused over the region of interest and lower resolution is on the opposite side of the earth. To eliminate potential errors that could occur in the lowest resolution regions, the model solution is weighted heavily towards the solution of a global model of uniform resolution. Both models had their highest resolution, of between 50 and 60 km, centred on Australia (see Figure 7). Outside this region, the CC-Mk2 model solutions were nudged towards those of a CSIRO Mark 2 A2 simulation and the CC-Mk3 model solutions were nudged towards the simulation of a CSIRO Mark 3 A2 model (see Table 2).

The analysis of wind conditions in the NCEP and climate model data sets was based upon the identification of the most extreme wind events that have occurred over the forty years from 1961 to 2000 over the region indicated in Figure 8. At each grid point daily wind speeds for this period were ranked and the greatest 1% of wind speeds (approximately 146 values per grid point) and their associated dates were stored. The dates of occurrence of extreme wind speeds within the region of interest were then pooled, and sorted into a list of dates for which patterns of MSLP could be synoptically typed.

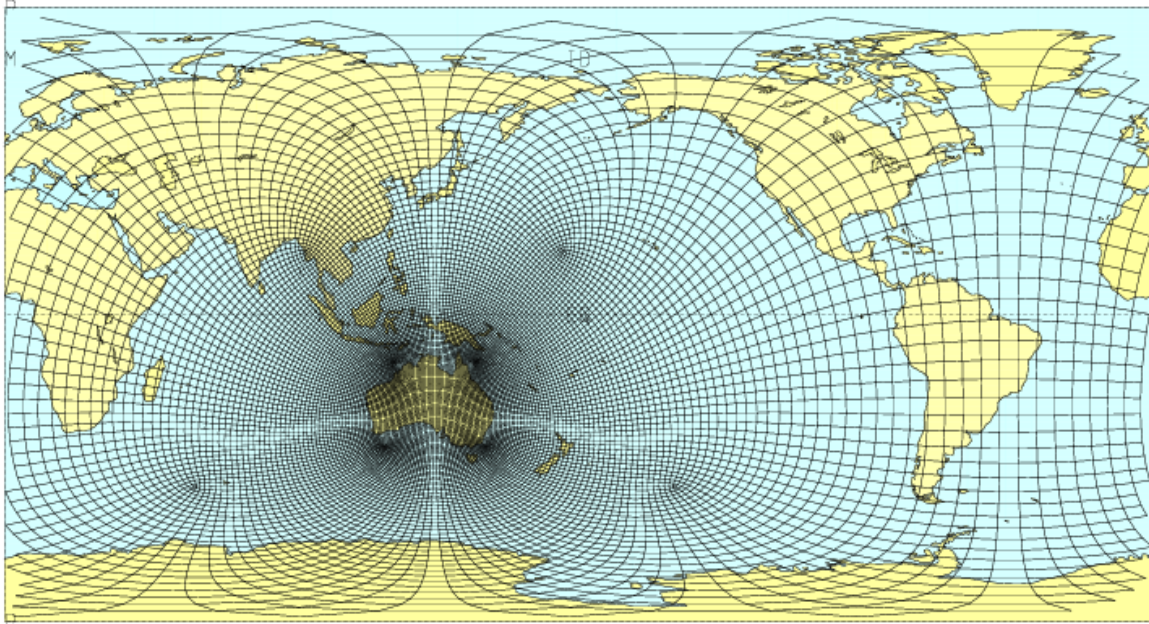


**Figure 7:** Diagram illustrating the stretched grid of the cubic conformal model.

Figure 8 shows the six gridpoints in the NCEP reanalyses that fall within the region of interest. The CC models with their finer spatial resolution had 76 gridpoints located in the region. This means that the models contributed a significantly larger pool of extreme wind events for synoptic classification. However, the large spatial scale of the severe synoptic systems ensured that large numbers of gridpoints register extreme winds on the same date. The number of events selected for synoptic typing from the NCEP reanalyses was around 400 while for the models, the number was approximately twice as large.

## 4.2 Extreme Wind Synoptic Weather Types

The strongest 1% of wind speed events in the region spanning 35°S to 45°S and 140°E to 160°E were selected from the 40 years of NCEP reanalyses. Figure 9 shows how these events are distributed between the months of the year. Approximately 70% of extreme wind days occur in the winter half year from May to October inclusive with 15% of those days occurring in August. January has the lowest number of extreme winds days.

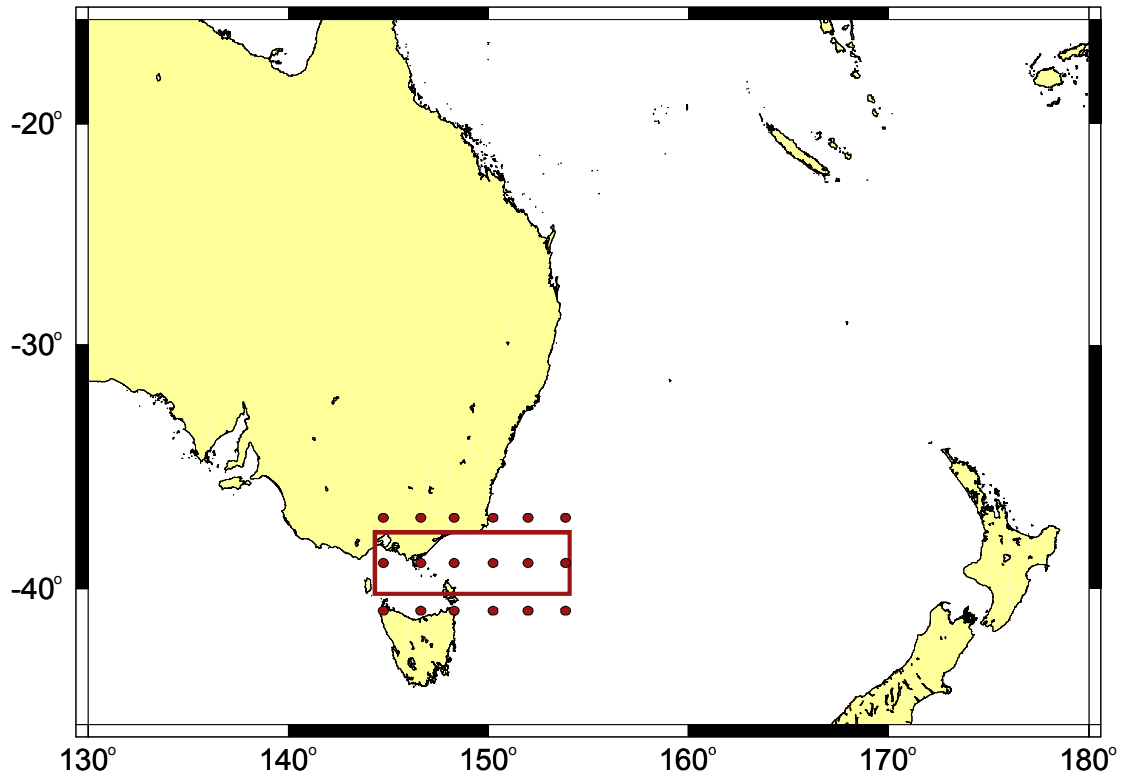


**Figure 8:** The region for which wind extremes from the NCEP reanalyses and the CSIRO climate models were analysed.

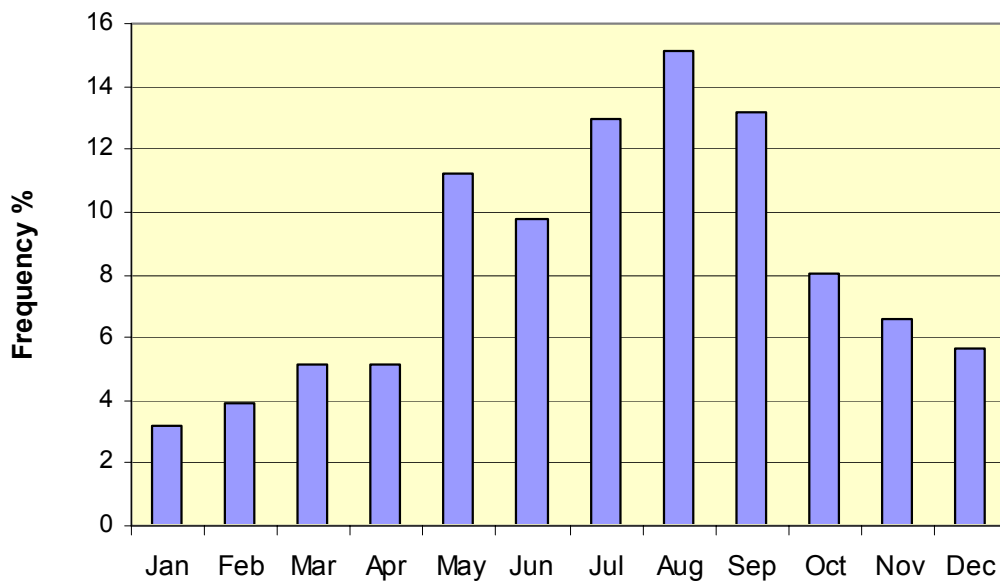


**Figure 9:** Frequency histogram of the number of days on which wind speeds equalled or exceeded that of the strongest 1% of all winds in the 1961 to 2000 NCEP reanalyses data.

The pressure patterns associated with the extreme wind days were analysed using a technique known as synoptic typing (see Yarnal, 1993). This is a correlation based typing technique in which fields are grouped based on Pearson product-moment correlations. Similar fields are identified on the basis of similar spatial structures (i.e. highs and lows in similar positions) with little emphasis on the magnitude of the patterns. The typing was carried out over the region bounded by 140 and 160°E and 35 and 45°S. More details of the typing procedure can be found in Appendix 1.

The typing procedure yielded the six synoptic patterns shown in Figure 10. The first three patterns are associated with the passage of cold fronts. The first pattern, accounting for 13% of extreme wind days, is characteristic of the pattern that precedes the arrival of a front with winds in the region of interest mainly from a northwesterly to westerly direction. With the arrival of the front, winds are generally from the west to southwest. This second pattern is associated with 34% of extreme wind days. Finally, the winds shift to a southwesterly direction as the front and associated depression move off to the east. The percentage of extreme wind days that are associated with this third, post-frontal, weather pattern is 22%. In total, 69% of extreme wind days are due to the passage of a front.

The next most prevalent synoptic pattern is the Tasman low in which a depression in the southern Tasman Sea brings winds from a predominantly southerly direction to Bass Strait. Tasman lows account for 23% of extreme wind days. On 6% of extreme wind days, the synoptic situation consisted of a cut-off low located to the east of the New South Wales coast and a ridge of high pressure in the southern Tasman Sea. Winds in Bass Strait are mainly southeasterly. The final synoptic weather pattern identified was that of a continental low centred over New South Wales and Victoria. Winds are generally from the east or northeast and as such would not be expected to cause storm surges. They account for only 2% of extreme wind days.

### **4.3 Extreme Sea Level Synoptic Weather Patterns**

Sea level records from two tide gauges along the Victorian coast were used to refine the relationship between extreme winds, sea levels and synoptic weather patterns. The locations of the two tide gauges define the western and eastern limits of the region of interest. The data from the Stony Point gauge was obtained from the National Tidal Centre of the Australian Bureau of Meteorology. The record extends from June 1993 onwards. The Lakes Entrance data was compiled from several tide gauges operating in Lakes Entrance since January 1974 (Grayson et al, 2004, Tan and Grayson, 2002).

In both data sets, sea level residuals, sea levels after the removal of the tidal signal, were used to identify days on which storm surges occurred. A daily maximum value of at least 0.4 m above mean sea level was used to denote a storm surge. This yielded 174 days for Stony Point and 184 days for Lakes Entrance. The MSLP patterns at 00 UTC on the identified days were then correlated against the MSLP patterns shown in Figure 10 to determine the relative proportions of each synoptic type responsible for elevated sea levels at the two locations. Results are shown in Table 3. Synoptic weather patterns associated with the passage of cold fronts account for almost all storm surges at Stony Point. Tasman low pressure systems account for 1% of events and 3% of events could not be matched to any of the six patterns. At Lakes Entrance, storm surges occur mainly during frontal events particularly when the pattern is frontal or post-frontal. Elevated sea levels due to Tasman lows occur on 23% of days, cut-off lows account for 3% of days and 1% of days remained unclassified. As expected, since the wind direction is not conducive to storm surge generation, continental lows do not produce elevated sea levels at either location.

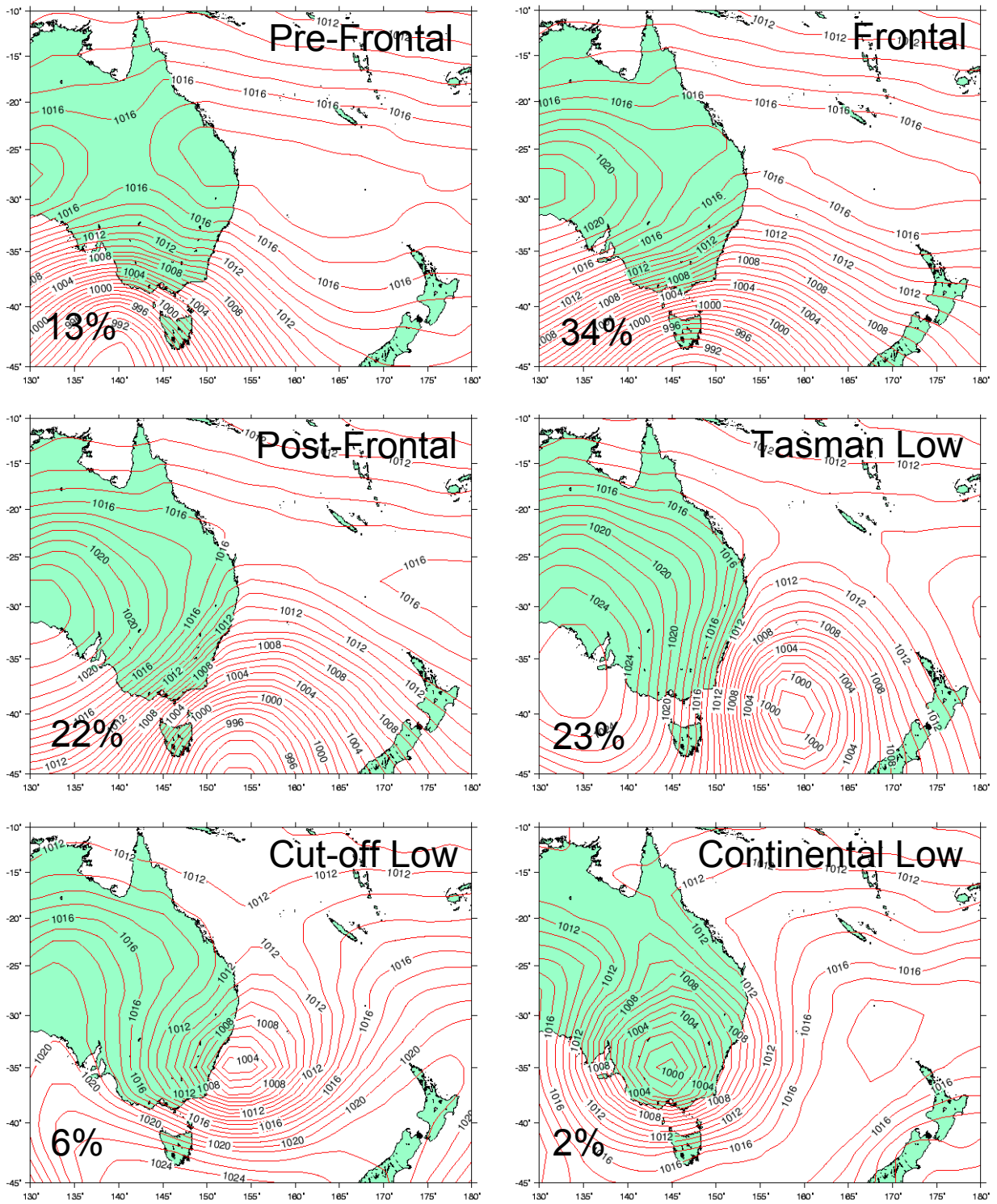
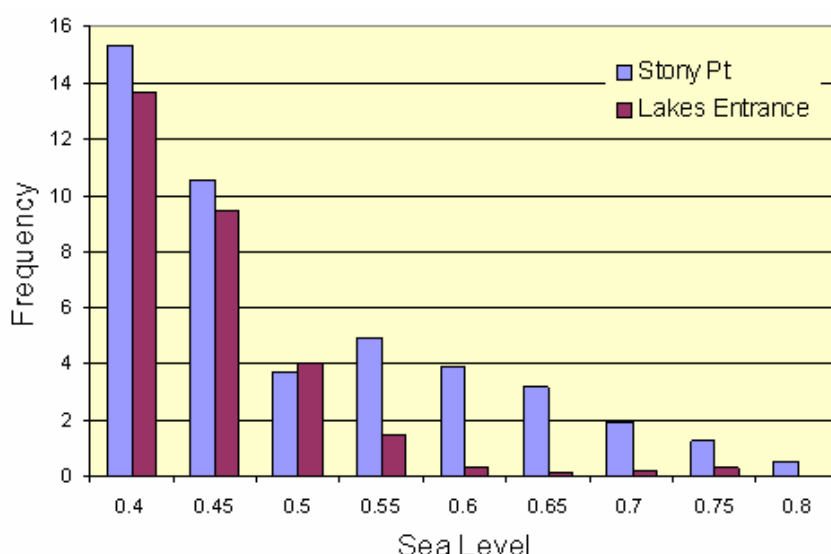


Figure 10: The synoptic types responsible for extreme wind days.

**Table 3:** The percentages of extreme wind days and storm surge days associated with each synoptic type.

Type	Name	Extreme Wind Days	Stony Point storm surge days	Lakes Entrance storm surge days
1	Pre-frontal	13	31	6
2	Frontal	34	43	36
3	Post-frontal	22	22	29
4	Tasman Low	23	1	23
5	Cut-off low	6	0	3
6	Continental low	2	0	0
U	Unclassified	0	3	1

The average annual frequency of storm surge days was evaluated for the two tide gauge locations after missing data was taken into account. At Stony Point approximately 27 days per year registered sea level residuals above 0.4m while at Lakes Entrance there were about 15 storm surge days per year. Event duration varies from a day to several days depending on the speed and intensity of the associated pressure system. The frequency distribution of sea level residuals from 0 to 0.8 m is shown in Figure 11.



**Figure 11:** Frequency of storm surge days in each sea level residual category.

#### 4.4 The Impact of Climate Change

A CC-Mk2 and a CC-Mk3 regional climate simulation are used to determine how climate change is likely to affect the behaviour of the different patterns associated with storm surges in the future. To begin with, the performance of the two models is assessed by examining the proportions of synoptic patterns that arise when extreme wind days are identified in the output of a 1961 to 2000 simulation using the same method that was used for the NCEP reanalysis data. The results are presented in Table 4. Note that for ease of interpretation, the three stages of frontal passage have been summed to produce a single frontal class.

A comparison of the CC-Mk2 and reanalysis results shows that the relative frequencies of MSLP patterns that produce extreme wind speeds in the model have been captured reasonably realistically, although there is a tendency for a greater number of frontal situations and fewer Tasman lows. The performance of the CC-Mk3 model on the other hand, is less realistic with both Tasman and cut-off lows patterns considerably underestimated in frequency and frontal situations and continental lows overestimated. More detailed analysis of the performance of this model over the central east coast of Australia in Abbs and McInnes (2004) and Hennessy et al (2004) has revealed that the poorer performance of the CC-Mk3 model is related to the influence of the Mark 3 global model from which CC-Mk3 obtains its boundary forcing. The Mark 3 global model has been found to have a more zonal global pressure pattern, relative to observations, leading to a more frequent occurrence of westerly winds along the south coast of Australia. This is thought to be related to a cool bias in sea surface temperatures off the east coast of the continent. Despite the improved spatial resolution and the correction of the cool bias in the CC-Mk3 model the model performance was not found to improve significantly. Clearly the boundary forcing provided by the Mark 3 global model dominates the synoptic patterns that evolve in the higher resolution CC model.

**Table 4:** Percentages of extreme wind days associated with each synoptic type for 1961 – 2000, 2030 and 2070 climates.

Name	Reanalysis Data	1961 – 2000 Reference Period		2030		2070	
		CC-Mk2	CC-Mk3	CC-Mk2	CC-Mk3	CC-Mk2	CC-Mk3
Frontal	69	72	86	77	83	79	82
Tasman low	23	17	3	15	3	16	3
Cut-off low	6	6	2	4	1	3	3
Continental low	2	3	6	3	7	1	6
Unclassified	0	1	4	1	5	1	5

The application of the synoptic typing procedure to extreme wind days identified in 40 year model simulations centred on 2030 and 2070 yields the percentages of the various synoptic types presented in Table 4. The proportion of frontal wind days increases in the output of CC-Mk2 from 72% for the reference period to 77% in 2030 and 79% in 2070. Cut-off lows, on the other hand, decline in frequency from 6% to 4% in 2030 and to 3% in 2070. Tasman lows also decline slightly in frequency from 17% to 16% in 2070. In the output of the CC-Mk3 model, frontal conditions are found to decrease slightly in frequency from 86% over the reference period to 83% in 2030 and 82% in 2070 while cut-off lows show a small increase in number.

## 5 Summary

This report provides an analysis of possible future changes in mean and extreme wind speeds over eastern Victoria. Results from a total of thirteen global and regional climate models are incorporated in the projections given to provide an indication of the uncertainty associated with the results. The ranges of change presented will be used to provide limits on the changes that could occur to wind forcing of storm surges in the second stage of this study. In this second stage the projections and the analysis of the synoptic patterns responsible for extreme wind events and, more particularly, storm surges will provide the basis for the provision of atmospheric data with which to force a hydrodynamic storm surge model.

## **Acknowledgments**

The work of the authors draws upon research findings of many colleagues within CSIRO Marine and Atmospheric Research and overseas research institutions. CSIRO global and regional climate models were developed by the members of the Climate, Weather and Ocean Prediction Theme of CSIRO Marine and Atmospheric Research.

Tide gauge data have been provided by the National Tidal Centre of the Australian Bureau of Meteorology and by Rodger Grayson and Kim Seong Tan of the University of Melbourne. Part of this work was funded by the Australian Greenhouse Office through the Australian Climate change Research Program.

## References

- Abbs, D.J., and McInnes, K.L., 2004: The impact of climate change on extreme rainfall and coastal sea levels over south-east Queensland. Part 1: Analysis of Extreme Rainfall and Wind Events in a GCM. Report to Gold Coast City Council. 47pp.
- Grayson, R.B., Candy, R., Tan, K.S., McMaster, M., Chiew, F., Provis, D., and Zhou, S., 2004: Gippsland Lakes Flood Level Modelling Project Final Report. University of Melbourne Centre for Environmental Applied Hydrology Report.
- Hennessy, K.J., Page, C.M., McInnes, K.L., Jones, R.N., Bathols, J., Collins, D., and Jones, D., 2004a: Climate Change in New South Wales Part 1: Past climate variability and projected changes in average climate. CSIRO Report for the New South Wales Greenhouse Office. 46pp.
- Hennessy, K.J., McInnes, K.L., Abbs, D.J., Jones, R.N., Bathols, J., Suppiah, R., Ricketts, J., Rafter, T., Collins, D., and Jones, D., 2004b: Climate Change in New South Wales Part 2: Projected changes in climate extremes. CSIRO Report for the New South Wales Greenhouse Office. 79pp.
- Hubbert, G.D., and McInnes, K.L., 1999: A storm surge inundation model for coastal planning and impact studies., *J. Coastal Research*, 15,168-185.
- IPCC 2000 [Nakicenovic, N., and Swart, R., (eds)]: Special Report on Emissions Scenarios, Cambridge University Press, Cambridge, 612pp.
- McInnes, K.L. and Hubbert, G.D., 2003: A numerical modelling study of storm surges in Bass Strait. *Aust. Met. Mag.*, 52, 143-156.
- McInnes, K.L., Walsh, K.J.E., Hubbert, G.D., and Beer, T., 2003: Impact of Sea-level Rise and Storm Surges on a Coastal Community. *Nat. Haz.*, 30(2), 187-207.
- Tan, K.S., and Grayson, R.B., 2002: Reconstruction of coastal ocean levels offshore of Lakes Entrance for the Gippsland Lakes Flood Modelling Project. University of Melbourne Centre for Environmental Applied Hydrology Report.
- Whetton, P.H., England, M.H., O'Farrell, S.P., Watterson, I.G., and Pittock, A.B., 1996: Global comparison of the regional rainfall results of enhanced greenhouse coupled and mixed layer ocean experiments: Implications for climate change scenario development. *Climatic Change*, 33(4), 497-519.
- Whetton, P.H., McInnes, K.L., Jones, R.N., Hennessy, K.J., Suppiah, R., Page, C.M., Bathols, J., and Durack, P., In preparation: Climate change projections for Australia for impact assessment and policy application: A review. CSIRO Technical Paper.
- Yarnal, B., 1993: *Synoptic Climatology in Environmental Analysis: A Primer*. Belhaven Press, London.

## Appendix 1 – Synoptic Typing

The synoptic typing procedure follows the method of Yarnal (1993) and is a correlation based pattern-typing technique in which fields of gridded numerical data are grouped based on Pearson product-moment correlations. Similar fields are identified on the basis of similar spatial structures (i.e. highs and lows in similar positions) with little emphasis on the magnitude of the patterns.

To establish a synoptic climatology compatible with the output from the climate models, this technique was first applied to 00 UTC MSLP reanalysis fields valid for the extreme wind days. These fields spanned the region between 140 and 160°E and 35 and 45°S and contained 64 (6x6) gridpoints. The following steps were then applied to the data set.

Each MSLP field is normalised:

$$Z_i = \frac{x_i - \bar{X}}{s}$$

where  $Z_i$  is the normalised value at a grid-point  $i$ ,  $x_i$  is the initial value at gridpoint  $i$ ,  $\bar{X}$  is the mean of  $X_{i=1 \text{ to } N}$  where  $N$  is the number of grid points and  $s$  is the standard deviation of  $X_{i=1 \text{ to } N}$ . The effect of this normalisation is to eliminate the seasonal impact on pressure pattern intensity, thus permitting direct inter-seasonal comparisons.

Once normalised, each field in the extreme wind days data set is compared with all of the other fields in the data set using Pearson product-moment correlations ( $r_{xy}$ ).

$$r_{xy} = \frac{\sum_{i=1}^N [(x_i - \bar{X})(y_i - \bar{Y})]}{\sqrt{\sum_{i=1}^N (x_i - \bar{X})^2 \sum_{i=1}^N (y_i - \bar{Y})^2}}$$

In this formula,  $x_i$  and  $y_i$  represent the values at each of the  $N$  grid points in the two fields being compared.  $\bar{X}$  and  $\bar{Y}$  represent the means of the values in the two fields. Pairs of MSLP fields are considered similar if  $r_{xy} \geq 0.7$ . Yarnal (1993) discusses the numerous sources of subjectivity in choosing a correlation threshold. The value of 0.7 was chosen after experimentation showed that it provided an acceptable balance between the number of patterns produced and the number of days that were not classified.

Once all of the fields have been compared with all of the other fields in the data set, the field with the largest numbers of  $r_{xy}$  values meeting the threshold criteria is designated “key pattern” 1 and is considered representative of the first field type. This “key pattern” as well as all the fields with which it is considered to be similar are then removed from the analysis. All fields deemed to be similar to each of those fields are also removed. The analysis is then repeated with the reduced data set to find “key pattern 2”, and so on, until all fields are classified into  $m$  groups of 3 patterns or more. The remainder are considered unclassified.

Once the “key patterns” are established, a second pass over the entire data set is made. This is necessary because it is possible for any particular field to be significantly correlated with more than one pattern. In this step, each field is assigned the “key pattern” with which it is most highly correlated. A second pass was also made over the unclassified fields to assign them to one of the identified “key patterns” A correlation threshold of 0.5 was chosen for this step.